LA-UR- 95-4362

CONF-951202--1

Title: Ion beam analysis of $MgAl_2O_4$ spinel irradiated with fast neutrons to 50-250 dpa

Author(s): Ning Yu, Carl J. Maggiore, Kurt E. Sickafus, Michael Nastasi, Frank A. Garner, Glenn W. Hollenberg, and Richard C. Bradt

Submitted to: J. Nuclear Materials (1995)

Los Alamos
NATIONAL LABORATORY

Ion beam analysis of $MgAl_2O_4$ spinel irradiated with fast neutrons to 50-250 dpa

Ning Yu [a], Carl J. Maggiore [a], Kurt E. Sickafus [a], Michael Nastasi [a],
Frank A. Garner [b], Glenn W. Hollenberg [b], and Richard C. Bradt [c]

[a] Materials Science and Technology Division, Los Alamos National Laboratory, Los Alamos, NM 87545, USA

[b] Materials Science Department, Pacific Northwest Laboratory, Richland, WA 99352, USA

[c] Metallurgical and Materials Engineering, University of Alabama, Tuscaloosa, AL 35487, USA

Abstract

Non-destructive ion beam analysis techniques have been employed to examine the radiation damage in $MgAl_2O_4$ spinel single crystals irradiated with fast neutrons at 400 and 750 °C to high fluences ($\geq 5x10^{22}$ n/cm^2, $E_n > 0.1$ MeV). Rutherford backscattering and ion channeling measurements using 1-4 MeV He ion beams revealed that the radiation damage saturated after irradiation at 400 °C to 50 displacements per atom. The energy dependence of dechanneling indicated the dominant extended defects present in the highly irradiated spinel are in the form of dislocations. Channeling angular scans of particle induced x-ray emission further suggested that neutron irradiation tends to randomize cation distribution for Mg^{2+} and Al^{3+} cations on the lattice sites. These results are compared to the microstructure observations of Kinoshita, *et al.* and the neutron scattering results of Sickafus, *et al.*

To be presented at the 1995 Fall Meeting of the Japan Institute of Metals, in the Session of Lattice Defects and Radiation-Induced Phenomena, Honolulu, Hawaii, December, 1995,
and to be published in J. Nucl. Mater.

Key Words: $MgAl_2O_4$ spinel, Ceramic, Fast neutron irradiation, Dislocation, Cation disorder, Ion beam analysis, RBS, PIXE, Ion Channeling.

1. Introduction

Radiation resistant ceramics with good electrical insulation and mechanical and optical properties are desired for applications in radiation environments. Among the studied ceramics, stoichiometric magnesium aluminate spinel ($MgAl_2O_4$) exhibits impressive resistance to void formation and amorphization. Previous studies have shown that spinel retained its ordered cubic crystalline structure with negligible swelling under fast neutron irradiation [1-5] and ion irradiation [6-10] at elevated temperatures (> 25 °C). Transmission electron microscopy (TEM) revealed that the primary form of retained damage was faulted interstitial dislocation loops lying on (110) and (111) habit planes [3] as well as rosette dislocation configurations [3,5]. A dislocation density analysis of Zinkle [8] indicated that the number of interstitials retained in the form of dislocation loops is only 0.03-0.12 at.% of the total number of displacements experienced during the irradiation, up to 35 displacements per atom (dpa).

The recombination of interstitials and vacancies is believed to be the predominant mechanism for annihilation of the point defects generated by displacement irradiation [1]. The negligible effect of void swelling in spinel is attributed to the absence of an unfaulting mechanism to assist loop growth [3]. However, some recent studies [11-15] have shown that spinel can be amorphized by ion irradiation at cryogenic temperatures where point defect mobility is minimized. It has been observed that spinel undergoes a two-stage phase transformation process under ion-irradiation: (1) from the ordinary spinel phase to a metastable crystalline phase; and (2) from this crystalline phase to an amorphous phase [11,15]. Nano-indentation measurements demonstrate that formation of the metastable crystalline phase is accompanied by an increase in the elastic modulus, while substantial elastic softening occurs upon amorphization [15]. However, similar ion irradiations at elevated temperatures do not induce such phase transformations [16]. These observations in conjunction with previous studies indicate that the radiation response of spinel is irradiation temperature dependent.

Spinel is also one of the few oxides that have been irradiated in fission reactors with fast neutrons to extremely high fluences, 50-250 dpa [17]. Recently, these highly irradiated spinel specimens became available for characterization to understand the radiation damage phenomena. The first results of Garner, *et al.* [18] and Black, *et al.* [19] have shown that although the specimens darken significantly, there are no measurable changes in dimensions, physical integrity,

mechanical and elastic properties. Using neutron scattering techniques, Sickafus, *et al.* [20] have revealed that these neutron irradiated spinel specimens have a high degree of cation disorder and the Mg^{2+} and Al^{3+} cations are randomly distributed over all allowed octahedral and tetrahedral sites. This indicates that cation disorder is the largest retained damage in irradiated spinel. The recent microstructure study of Kinoshita, *et al.* [21] showed that the predominant defect structure following irradiation at 400 °C to 22 dpa consists of 1/4[110] type interstitial loops on the (111) and (110) planes. Irradiation at 750 °C to damage levels of 56-217 dpa induces stacking fault networks, along with a very low density of small voids ($\leq$ 8 nm) that account for void swelling of only 0.07% volume fraction.

In this study, we have used ion beam analysis techniques to examine the radiation damage in these neutron irradiated $MgAl_2O_4$ spinel single crystals. Saturated lattice disorder has been observed for irradiation at 400 °C to 50 dpa. Dechanneling from the lattice disorder has been found to be proportional to the square root of the He incident energy. This reveals that dislocations are the dominant extended defects present in the highly irradiated spinel [22]. Channeling angular scans further indicated that Mg^{2+} and Al^{3+} cations tend to switch lattice sites and cation distribution becomes randomized under neutron irradiation. These observations are compared with the microstructure observations of Kinoshita, *et al.* [21] and the neutron scattering data of Sickafus, *et al* [20].

2. Experiment

Synthetic single-crystal $MgAl_2O_4$ specimens were prepared from the same rod into cylindrical pellets with dimensions of 5 mm diameter and 2-3 mm thickness. The specimens were (001) orientation with one-side polished to an optical finish. Four specimens were irradiated in the Materials Open Test Assembly (MOTA) of the Fast Flux Test Facility (FFTF) with fast neutrons ($E_n > 0.1$ MeV) under nominal irradiation conditions of 5.3×10^{22} and 2.49×10^{23} n/cm^2 at 400 °C, and 5.6×10^{22} and 1.37×10^{23} n/cm^2 at 750 °C, respectively. At the end of irradiation cycles, the specimens quickly cooled to 370 °C due to the absence of gamma-ray heating. One specimen was not irradiated but stored at room temperature as a reference. The details of specimens and irradiation conditions can be found elsewhere [17]. The specimens used in this study are specified in Table 1. The radiation damage levels experienced by the specimens can be estimated using a

rough conversion factor of 1 dpa per $1x10^{21}$ ($E_n > 0.1$ MeV) [17] under the assumption of 27 and 30 eV as threshold displacement energies for cations and anions.

The radiation induced lattice damage in spinel was measured with Rutherford backscattering and ion channeling (RBS/C) along the <100> axial channeling direction using 1-4 MeV He^+ ion beams. Dechanneling rates as a function of incident He beam energy were determined to understand the nature of the defects present in the irradiated samples. According to the theoretical work of Mory and Quere [22] and the measurements of Picraux, *et al* [23,24], the dechanneling caused by dislocations is proportional to $E^{1/2}$, where E is the incident beam energy. Determination of radiation damage in Mg and Al cation sublattices is limited in RBS measurements where the Mg backscattering signal merges into the Al signal. Particle induced x-ray emission (PIXE) using a 2 MeV He ion beam was employed to differentiate Mg and Al signals. In conjunction with ion channeling angular scan techniques, PIXE measurements provide insights into the cation disorder in spinel.

3. Results

Figure 1 shows aligned RBS spectra for 2 MeV He ions from $MgAl_2O_4$ spinel samples along the <100> axis before and after fast neutron irradiation at 400 °C to 50 and 250 dpa. Good single-crystal quality of the unirradiated specimen is indicated by low channeling yields and distinct surface peaks for the Al, Mg, and O signals as compared to the random spectrum. A minimum yield is defined as the ratio of the backscattering yield of an aligned spectrum to that of a random spectrum. The minimum yield of 3.4% for the Al signal is obtained near the surface of the pristine specimen. Following neutron irradiations, aligned spectra exhibit higher dechanneling yields for the Al, Mg, and O signals, indicating the presence of radiation-induced lattice damage. The dechanneling rate increases with increasing depth below the surface. This is due to the integrated dechanneling effect of the lattice damage on the initially well channeled He ion beam along its trajectory. The average minimum yield for the Al over the top 80 nm thickness increases from 3.4% to 32% following the irradiation to 50 dpa. It is interesting to note, from the RBS/C results, that the accumulated radiation damage reaches a saturation level at a dose of 50 dpa. No further increase in the dechanneling yield is observed as the neutron dose significantly increases from 50 to 250 dpa.

Fig. 2 shows aligned RBS spectra for 2 MeV He ions from $MgAl_2O_4$ samples before and after the irradiations at 750 °C to 50 and 140 dpa. The radiation induced disorder is indicated by the higher dechanneling rates in comparison to those of the pristine specimen. The surface peaks are still visible in the aligned spectrum after irradiation to 50 dpa and the minimum yield appears to be 6.5% near the surface region of 80 nm thickness. More radiation damage accumulates in the spinel as the irradiation dose increases from 50 to 140 dpa, as shown by the higher minimum yield, 10%. The increase in dechanneling indicates the evidence that the lattice damage does not reach a saturation level at least for a dose of 50 dpa. It is uncertain whether the damage level for 140 dpa represents a saturation. However, it is important to note by comparing Fig. 2 with Fig. 1, that the damage levels observed on the samples irradiated at 750 °C are lower than those of 400 °C. This demonstrates that spinel is more susceptible to neutron induced damage at lower irradiation temperatures.

The channeling results given in Figs. 1 and 2 provide no direct information on the type of defects present in the neutron irradiated spinel. However, measuring the incident energy dependence of dechanneling is a non-destructive means to gain some insight into the nature of the defect structure. Fig. 3 shows <100> aligned RBS spectra for 1 MeV He ions from three spinel samples: unirradiated and irradiated at 400 °C to 250 dpa or at 750 °C to 140 dpa. It is noticeable that the dechanneling yields from the irradiated specimens are considerably lower than those obtained using a 2 MeV He beam and shown in Figs. 1 and 2. In contrast, the channeling spectrum from the pristine specimen shows no sign of drastic changes as the He beam energy is reduced from 2 to 1 MeV, for a similar minimum yield is obtained. The influence of beam energy on the dechanneling rate in the irradiated specimens is further displayed in Fig. 4 where the aligned RBS spectra for 4 MeV He ions from the same samples are given. Enhanced dechanneling is evident for the incident He beam energy at 4 MeV versus 2 MeV. This energy dependence of dechanneling reveals that a certain type of defects may contribute to the observed dechanneling behavior.

A dechanneling parameter can be deduced from the measured RBS/C data in order to quantify the dechanneling behavior. Following the methodology of Picraux, *et al.* [23,24], the dechanneling parameter is defined as $ln[(1-X_d)/(1-X_v)$, where X_d and X_v are the minimum yields obtained from a disordered and a virgin crystal at a fixed depth. The values of dechanneling

parameter are evaluated from the RBS spectra in Figs. 1-4 for the Al signal alone at the depth around 40 nm and plotted versus $E^{1/2}$ in Fig. 5, where E is the incident beam energy. It is obvious that the dechanneling rate increases with increasing depth in the irradiated spinel. The data for the Al RBS signal were chosen to avoid the Mg and Al overlapping signals which resulted from two different depths with different dechanneling rates. A reasonably good linear relationship between the dechanneling parameter and $E^{1/2}$ is observed in Fig. 5 for the $MgAl_2O_4$ samples irradiated at 400 °C to 250 dpa or at 750 °C to 140 dpa. Based on previous theoretical prediction [22] and the experimental confirmation [23,24], the dechanneling that results from lattice distortions due to dislocations of either edge or screw character should follow the power law of $E^{1/2}$. Therefore, the linear relation observed in Fig. 5 indicates that the dislocations are the dominant extended defects causing the dechanneling. The higher values of dechanneling parameter in the specimen irradiated at 400 °C represent a higher concentration of dislocations as compared to the specimen of 750 °C.

In addition to the extended defects measurements, channeling is also useful to detect relative changes in lattice location for Mg and Al cations in spinel. Due to the small mass difference between Mg and Al, it is difficult to differentiate the Mg signal from the higher Al background in the RBS spectra. PIXE techniques provide a solution to this problem. Fig. 6 shows aligned and random PIXE spectra for 2 MeV He ions from an unirradiated spinel crystal. The x-ray fluorescence signals emitted from Mg and Al are well separated in the PIXE spectrum. The Mg and Al peaks are centered at the energies of 1.25 and 1.49 keV with partial overlap on the edge. The overlap is due to the limited energy resolution of the x-ray detector. The area under each peak of the Gaussian distribution represents the total intensity of x-ray fluorescence from each species in a probing depth of 4 μm. Fig. 6 clearly shows that as the incident He beam changes its alignment from the random direction to the <100> channeling direction, the PIXE yields drop by 10-fold. This indicates high quality of the unirradiated spinel crystal.

Fig. 7 shows <100> aligned and random PIXE spectra for 2 MeV He ions from $MgAl_2O_4$ samples irradiated at 750 °C to 140 dpa. Small reduction in the PIXE yields for the aligned spectrum relative to the random spectrum corresponds to the partial channeling for the incident He beam in a disordered crystal. Similar to the case of RBS/C measurements, minimum yield can also be defined for PIXE channeling as the ratio of PIXE yield along the channeling direction to that along the random direction. A minimum yield of 55% is obtained for Al in Fig. 7 from the

irradiated specimen, while a 10% value is obtained in Fig. 6 from the pristine specimen. The higher PIXE minimum yield obtained from the pristine specimen is due to the greater probing depth as compared to RBS.

Ion channeling angular scans in conjunction with PIXE were performed on the spinel samples with and without fast neutron irradiation at 400 °C to 50 dpa. Fig. 8 shows the PIXE yields for Al and Mg, normalized by those obtained along a random direction, as a function of tilt angle with respect to the <100> axis. The yields at the bottom of the channeling dip curves represent the PIXE minimum yields. An axial half-angle, $\Psi_{1/2}$, is defined as the half width of the dip curve halfway between the minimum yield and the random yield. The dip curves for the pristine specimen show distinct differences between Al and Mg. The values of half-angle are found to be $0.40\pm0.01°$ and $0.30\pm0.01°$ for Al and Mg, respectively. The channeling dip becomes much shallower following the neutron irradiation, indicating the build-up of radiation damage. It is further noticeable that the dip curves for Al and Mg are less distinct. The half-angle values are 0.65° and 0.64° for Al and Mg, respectively. The broadening of the dip curve is a common effect in defective crystals because dechanneled particles have certain probability to be scattered into channeling directions. For normal spinel along the <100> axis, Al and Mg cations form separated atomic rows [25] with different atomic potentials that give rise to distinct half-angle values for Al and Mg. This is clearly observed in Fig. 8 prior to the irradiation. The reduction in the difference in the half-angle after the irradiation suggests that Al and Mg cations switch their occupied lattice sites and tend to distribute randomly over the lattice sites.

Fig. 9 depicts <100> channeling angular distributions for Mg and Al obtained from PIXE measurements on the spinel samples before and after irradiation at 750 °C to 50 dpa. As the radiation damage accumulates in the spinel crystal, the difference in the half-width of the angular scans for Al and Mg becomes less. The half-angle values of 0.46° and 0.43° are derived for Al and Mg, respectively. In comparison to Fig. 8, the dip in the angular scan curves appears to be deeper and the broadening is less. This is due to the fact that less damage is accumulated in the specimen irradiated at 750 °C. However, the reduced difference in the half-angle between Al and Mg after irradiation still suggests the tendency for randomization of Al and Mg cations on their lattice sites.

4. Discussion

The channeling study of highly irradiated spinel indicates that the defects causing pronounced dechanneling are substantially of a dislocation nature. This provides some additional support to the limited microstructure results reported for the similar high dose irradiated spinel samples [21]. Kinoshita, *et al.* [21] observed 1/4[110] type interstitial loops on the (111) and (110) planes in the spinel specimen irradiated at 400 °C to 22 dpa. They also found that this defect structure is similar to that observed in the spinel specimens, which were 'lightly' irradiated in the JOYO reactor in the neutron dose range 0.08-6.3 dpa. In the 'lightly' irradiated spinel samples, the average loop diameter increased with increasing irradiation temperature and neutron dose. These microstructure observations were also consistent with those of previous studies [1-5]. However, it is worth noting that stacking fault networks instead of dislocation loops were observed by Kinoshita, *et al.* in spinel irradiated at 750 °C to 56-217 dpa. It is known that the dechanneling resulting from stacking faults is insensitive to the incident beam energy [22]. The $E^{1/2}$ dependence of dechanneling behavior observed in Fig. 5 indicates that dislocations were present in the spinel specimen irradiated at 750 °C to 140 dpa. This inconsistency requires a further investigation.

RBS/C results in Fig. 1 clearly demonstrate that the lattice damage induced by neutron irradiation at 400 °C achieves a saturation level, as indicated by a minimum yield of 32% near the sample surface for a 2 MeV He beam. It is surprising that the degree of lattice disorder has no further increase with a huge increase in the irradiation dose from 50 to 250 dpa. Because the primary extended defects induced by irradiation at 400 °C are dislocation loops [21], the channeling data indicate that the loop formation is suppressed at a certain concentration level. In the irradiation dose range 0.08-6.3 dpa, the fraction of surviving defects that composed the loops was found to increase with increasing dose [21]. Therefore, based on this analysis, the defect concentration is expected to reach the saturation level at a dose between 6.3 and 50 dpa. The Xe ion irradiation in spinel crystals at 400 °C showed a similar dose range for damage saturation [26]. The comparison between Fig. 1 and Fig. 2 demonstrates that spinel is more resistant to radiation damage accumulation as the irradiation temperature increased from 400 to 700 °C. The channeling results in Fig. 2 showed that no damage saturation was reached at least to 50 dpa at 750 °C. It was unclear whether the damage level for 140 dpa represents saturation.

The channeling angular distributions in Figs. 8 and 9 suggest that Al and Mg cations have a tendency to switch lattice sites and distribute randomly over the lattice sites under neutron irradiation. Cation disorder is an important feature inherent in $MgAl_2O_4$ spinel that may contribute to the radiation resistance [20]. In normal spinel, Mg^{+2} and Al^{+3} ions occupy one-eighth of tetrahedral interstices and one-half of octahedral interstices, respectively, in a fcc anion framework. Cation disorder, the site exchange between Mg^{+2} and Al^{+3} ions, can be thermally activated at 800 °C and be frozen in by rapid quenching. Cation disorder with up to 30% of Mg^{+2} ions exchanging sites with Al^{+3} ions was observed in quenched spinel [27]. The neutron scattering study of Sickafus, *et al.* [20] demonstrated that fast neutron irradiation at 400 or 750 °C to 50 dpa induced 60% of Mg^{+2} ions to exchange sites with Al^{+3} ions [20]. This is equivalent to the complete randomization of the distribution of cations over all the allowed tetrahedral and octahedral interstices. The ion channeling results in Figs. 8 and 9 supported such a randomized cation configuration. Nevertheless, nuclear magnetic resonance using ^{27}Al magic angle spinning on these neutron irradiated spinel specimens suggested that Al was distributed nearly equally over the octahedral and tetrahedral sites, forming a nearly inverse spinel configuration [28]. The cause of two different conclusions is unclear at this stage.

The observations from this study along with other observations [20,21] reveal an important fact that the dominant microscopic changes in spinel induced by neutron irradiation involve formation of the interstitial loops and cation disorder. The cation sublattice disorder represents the largest retained damage ever measured in neutron irradiated spinel [20] as compared to other extended defects such as interstitial loops, stacking fault networks, and voids. We believe that cation disorder is an important mechanism for the annihilation of point defects and the storage of radiation damage. The existence of a large population of unoccupied interstices in spinel provides a route for cation site exchange and for interstitial-vacancy recombination following atomic displacement collisions. The calculation of Chen, *et al.* [29] using a shell potential model showed that the activation energy for the site exchange between Mg^{+2} and Al^{+3} is only 0.92 eV. The small activation energy supported these observations that cation disorder can be readily produced in spinel either thermally or by displacement irradiation.

5. Conclusions

Single crystal $MgAl_2O_4$ spinel specimens irradiated with fast neutrons at 400 and 750 °C to high fluences (50-250 dpa, $E_n > 0.1$ MeV) have been studied using RBS and PIXE in conjunction with ion channeling techniques. The $(Energy)^{1/2}$ dependence of dechanneling observed by RBS/C indicates that the dominant extended defects present in the highly irradiated spinel specimens are dislocations. RBS/C also has shown damage saturation in spinel after neutron irradiation at 400 °C to 50 dpa. This indicates that the formation of dislocations is suppressed at a certain concentration level. The PIXE channeling angular scans suggest that neutron irradiation tends to randomize the distribution of Mg^{2+} and Al^{3+} cations on the lattice sites. These observation are consistent with the microstructure observations of Kinoshita, *et al.* and the neutron scattering results of Sickafus, *et al.*

Acknowledgments

All ion beam work was performed at the Los Alamos Ion Beam Materials Laboratory. The research was sponsored by the U.S. Department of Energy, Office of Basic Energy Sciences, Division of Materials Sciences.

References

[1] L.W. Hobbs and F.W. Clinard, Jr., J. Phys. Colloque 41 (1980) C6-232.

[2] G.F. Hurley, J.C. Kennedy, F.W. Clinard, Jr., R.A. Youngman, and W.R. McDonell, J. Nucl. Mater. 103-104 (1981) 761.

[3] F.W. Clinard, Jr., G.F. Hurley, and L.W. Hobbs, J. Nucl. Mater. 108-109 (1982) 655.

[4] D.S. Tucker, T. Zocco, C.D. Kise, and J.C. Kennedy, J. Nucl. Mater. 141-143 (1986) 401.

[5] K. Nakai, K. Fukumoto, and C. Kinoshita, J. Nucl. Mater. 191-194 (1992) 630.

[6] P.A. Knight, M.L. Jenkins, and G.P. Pells, Mat. Res. Soc. Symp. Proc. 152 (1989) 135.

[7] G.P. Pells and M.J. Murphy, J. Nucl. Mater. 183 (1991) 137.

[8] S.J. Zinkle, J. Am. Ceram. Soc. 72 (1989) 1343.

[9] R. Yamada, S.J. Zinkle, and G.P. Pells, J. Nucl. Mater. 191-194 (1992) 640.

[10] S.J. Zinkle, Nucl. Instrum. Meth. B 91 (1994) 234.

[11] N. Yu, K.E. Sickafus, and M. Nastasi, Philos. Mag. Lett. 70 (1994) 235.

[12] N. Bordes, L.M. Wang, R.C. Ewing, and K.E. Sickafus, J. Mater. Res. 10 (1995) 981.

[13] K.E. Sickafus, N. Yu, R. Devanathan, and M. Nastasi, Nucl. Instrum. Meth. B (1995), in press.

[14] K.E. Sickafus, N. Yu, and M. Nastasi, Nucl. Instrum. Meth. B (1996), in press.

[15] N. Yu, R. Devanathan, K.E. Sickafus, and M. Nastasi, submitted to Phys. Rev. B (1995).

[16] N. Yu, K.E. Sickafus, and M. Nastasi, Mater. Res. Soc. Symp. Proc. 373 (1995) 401.

[17] F.A. Garner, G.W. Hollenberg, F.D. Hobbs, J.L Ryan, Z. Li, C.A. Black, and R.C. Bradt, J. Nucl. Mater. 212-215 (1994) 1087.

[18] F.A. Garner, G.W. Hollenberg, J.L Ryan, Z. Li, C.A. Black, and R.C. Bradt, in Fusion Reactor Materials Semiannual Progress Report DOE/ER-0313/15, (1993).

[19] C.A. Black, F.A. Garner, and R.C. Bradt, in Fusion Reactor Materials Semiannual Progress Report DOE/ER-0313/15, (1993).

[20] K.E. Sickafus, A.C. Larson, N. Yu, M. Nastasi, G.W. Hollenberg, F.A. Garner, and R.C. Bradt, J. Nucl. Mater. 219 (1995) 128.

[21] C. Kinoshita, K. Fukumoto, K. Fukuda, F.A. Garner, G.W. Hollenberg, J. Nucl. Mater. 219 (1995) 143.

[22] J. Mory and Y. Quere, Rad. Effects 13 (1972) 57.

[23] S.T. Picraux, D.M. Follstaedt, P. Baeri, S.U. Campisano, G. Foti, and E. Rimini, Rad. Effects 49 (1980) 75.

[24] S.T. Picraux, E. Rimini, G. Foti, and S.U. Campisano, Phys. Rev. B 18 (1978) 2078.

[25] W.R. Allen, J. Nucl. Mater. 199 (1993) 121.

[26] N. Yu, M. Nastasi, M.G. Hollander, C.R. Evans, C.J. Maggiore, K.E. Sickafus, and J.R. Tesmer, Mater. Res. Soc. Symp. Proc. 316 (1994) 69.

[27] U. Schmocker and F. Waldner, J. Phys. C 9 (1976) L235.

[28] E.A. Cooper, C.D. Hughes, W.L. Earl, K.E. Sickafus, G.W. Hollenberg, F.A. Garner, and R.C. Bradt, Mater. Res. Soc. Symp. Proc. 373 (1995) 413.

[29] S.P. Chen, M. Yan, J.D. Gale, R.W. Grimes, R. Devanathan, K.E. Sickafus, N. Yu, and M. Nastasi, Philos. Mag. Lett. (1995), in press.

Table 1 Single crystal specimens of $MgAl_2O_4$ spinel with and without fast neutron irradiations at FFTF.

Sample ID	Irradiation Temperature (°C)	Neutron Fluence (n/cm^2)	Estimated Damage Level (dpa)
100-3A	405	$5.3x10^{22}$	53
100-3B	385	$2.49x10^{23}$	249
100-4A	750	$5.6x10^{22}$	56
100-4B	750	$1.37x10^{23}$	137
100-4C	Reference	0	0

Figure Captions:

Fig. 1 Aligned RBS spectra for 2 MeV He ions from spinel samples along the <100> axis before and after fast neutron irradiations at 400 °C to 50 and 250 dpa, along with a random spectrum from the pristine sample.

Fig. 2 Aligned RBS spectra for 2 MeV He ions from spinel samples before and after fast neutron irradiations at 750 °C to 50 and 140 dpa, along with a random spectrum.

Fig. 3 Aligned RBS spectra for 1 MeV He ions from spinel samples before and after fast neutron irradiation at 400 °C to 250 dpa or at 750 °C to 140 dpa, along with a random spectrum.

Fig. 4 Aligned RBS spectra for 4 MeV He ions from spinel samples before and after fast neutron irradiation at 400 °C to 250 dpa or at 750 °C to 140 dpa, along with a random spectrum.

Fig. 5 Dechanneling parameter as a function of square root of incident He beam energy, from spinel samples irradiated with fast neutron at 400 °C to 250 dpa or at 750 °C to 140 dpa.

Fig. 6 Aligned and random PIXE spectra for 2 MeV He ions from the pristine spinel sample.

Fig. 7 Aligned and random PIXE spectra for 2 MeV He ions from the spinel sample irradiated with fast neutron at 750 °C to 140 dpa.

Fig. 8 PIXE angular distributions for Mg and Al from spinel samples before (solid line) and after (dashed line) fast neutron irradiation to 50 dpa at 400 °C.

Fig. 9 PIXE angular distributions for Mg and Al from spinel samples before (solid line) and after (dashed line) fast neutron irradiation to 50 dpa at 750 °C.

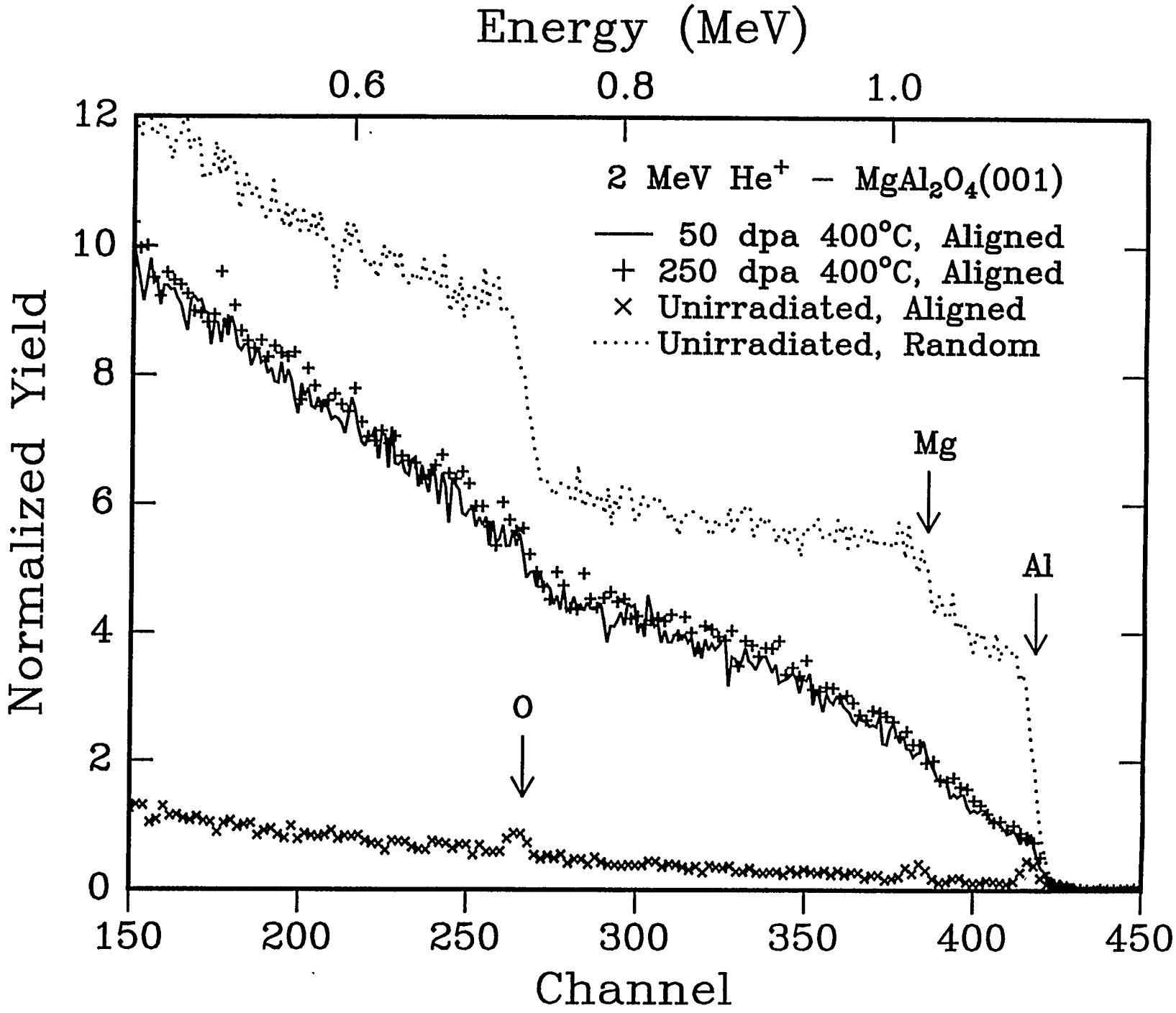
Energy (MeV)
0.6
0.8
1.0
12
10
8
6
4
2
0
Normalized Yield
2 MeV He+ – MgAl2O4(001)
50 dpa 400°C, Aligned
250 dpa 400°C, Aligned
Unirradiated, Aligned
Unirradiated, Random
Mg
Al
O
150
200
250
300
350
400
450
Channel

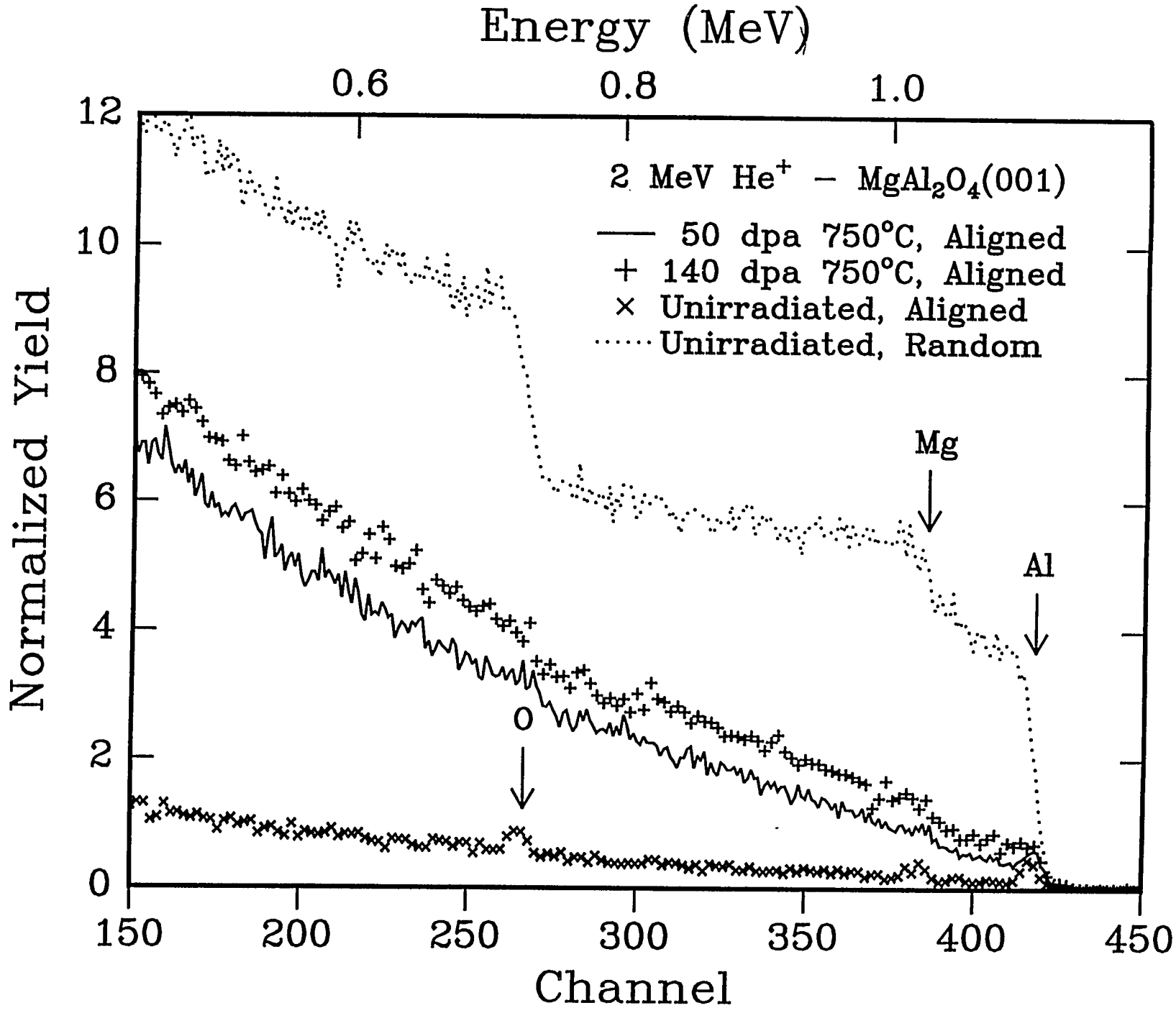
Energy (MeV)
0.6
0.8
1.0
12
10
8
6
4
2
0
Normalized Yield
2 MeV He+ – MgAl2O4(001)
50 dpa 750°C, Aligned
140 dpa 750°C, Aligned
Unirradiated, Aligned
Unirradiated, Random
Mg
Al
O
150
200
250
300
350
400
450
Channel

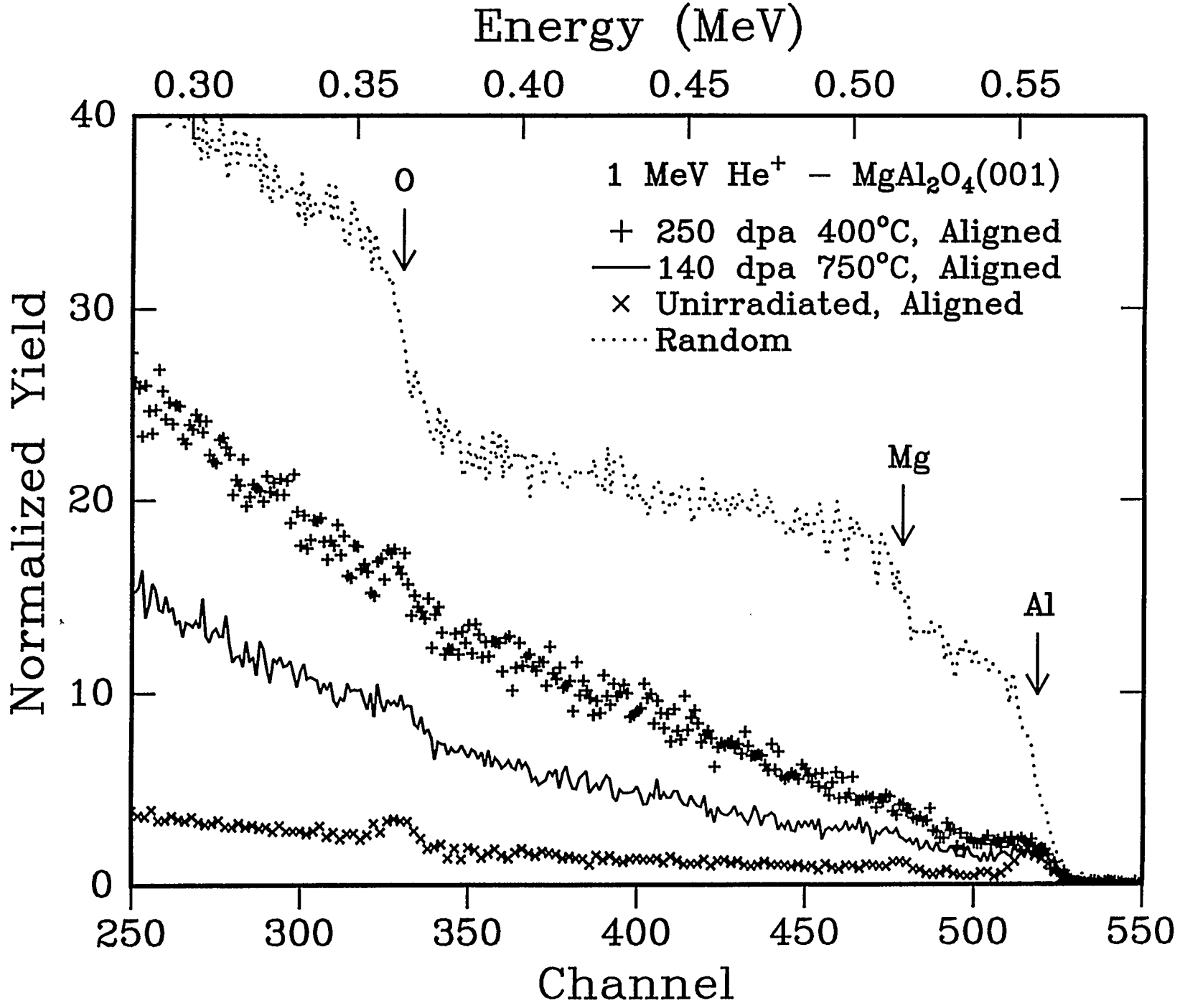
Energy (MeV)
0.30
0.35
0.40
0.45
0.50
0.55
Normalized Yield
40
30
20
10
0
1 MeV He+ – MgAl2O4(001)
+ 250 dpa 400°C, Aligned
140 dpa 750°C, Aligned
× Unirradiated, Aligned
Random
O
Mg
Al
250
300
350
400
450
500
550
Channel

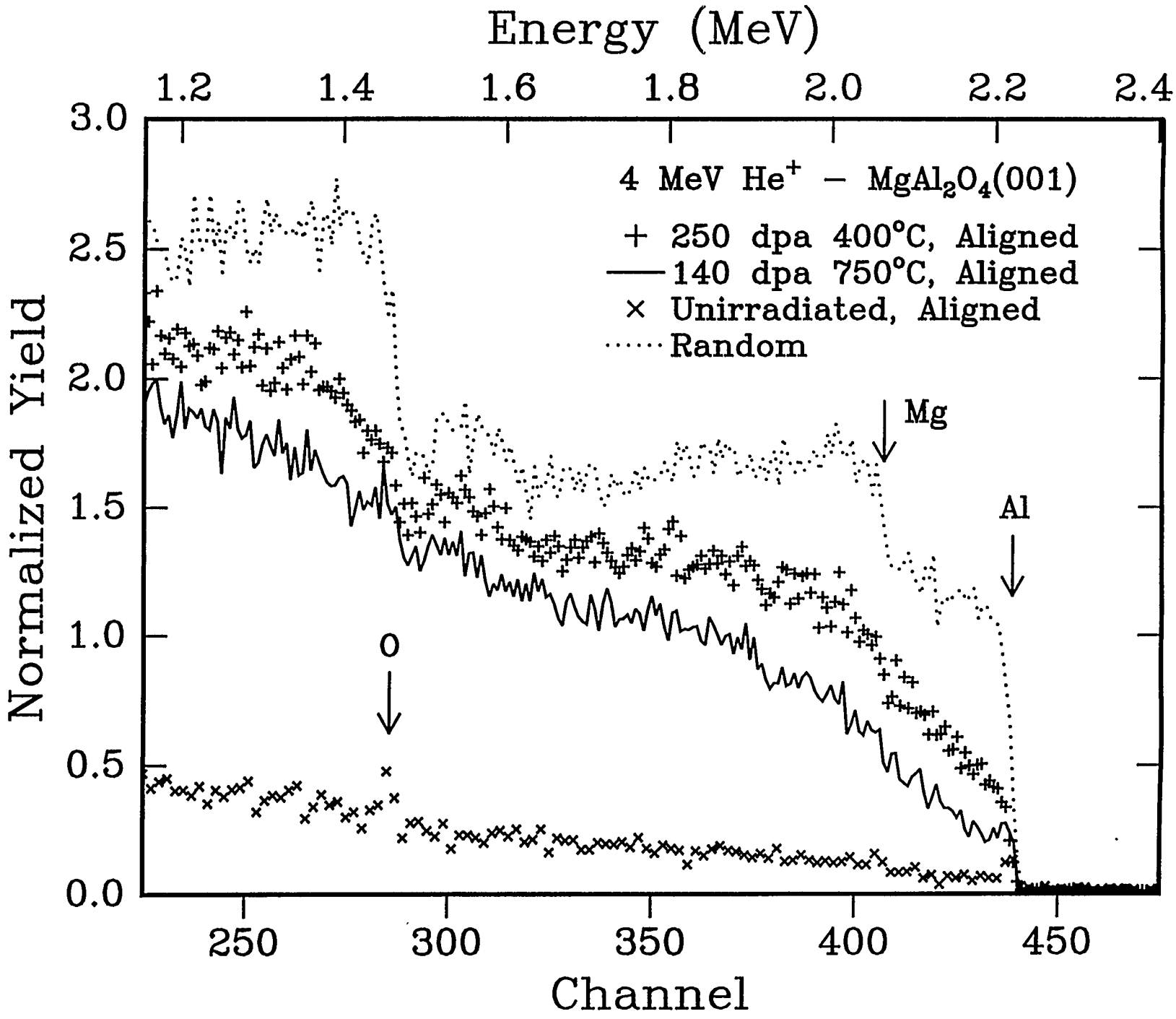
Energy (MeV)
1.2
1.4
1.6
1.8
2.0
2.2
2.4
3.0
2.5
2.0
1.5
1.0
0.5
0.0
Normalized Yield
4 MeV He+ – MgAl2O4(001)
+ 250 dpa 400°C, Aligned
140 dpa 750°C, Aligned
× Unirradiated, Aligned
Random
Mg
Al
O
250
300
350
400
450
Channel

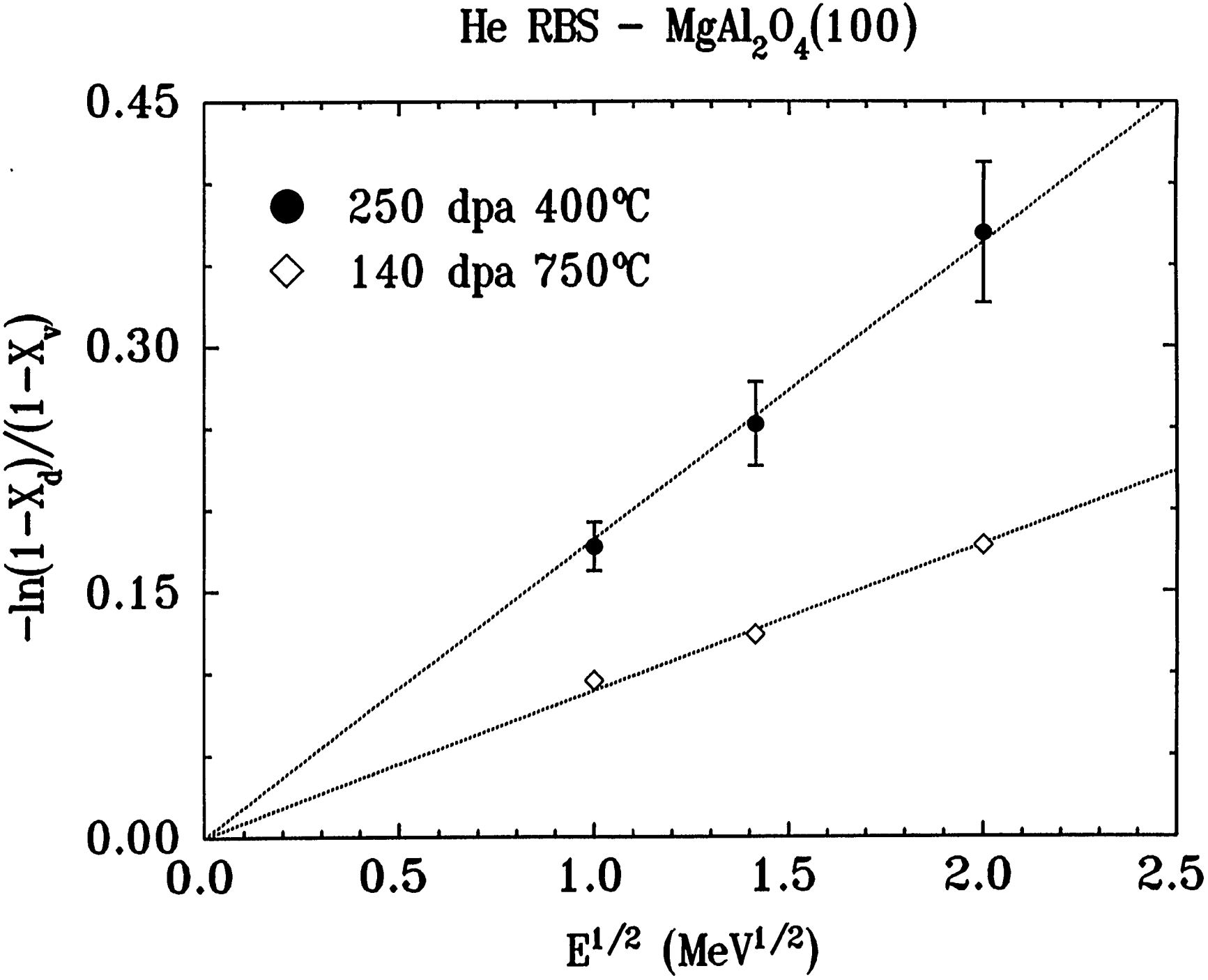
He RBS - $MgAl_2O_4$(100)
250 dpa 400℃
140 dpa 750℃
$-\ln(1-X_d)/(1-X_v)$
0.45
0.30
0.15
0.00
0.0
0.5
1.0
1.5
2.0
2.5
$E^{1/2}$ ($MeV^{1/2}$)

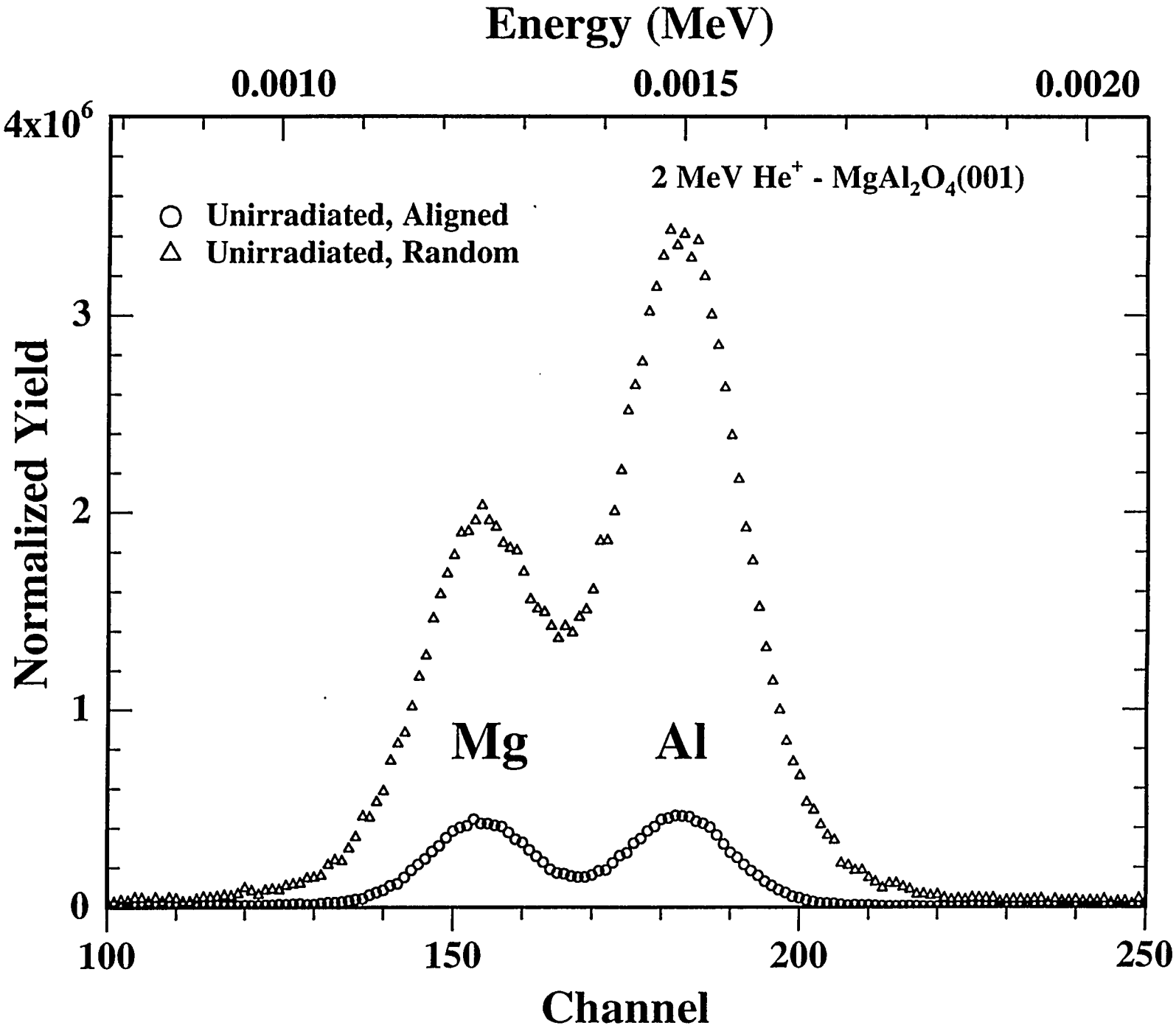
Energy (MeV)
0.0010
0.0015
0.0020
4x10^6
2 MeV He+ - MgAl2O4(001)
Unirradiated, Aligned
Unirradiated, Random
Normalized Yield
3
2
1
0
Mg
Al
100
150
200
250
Channel

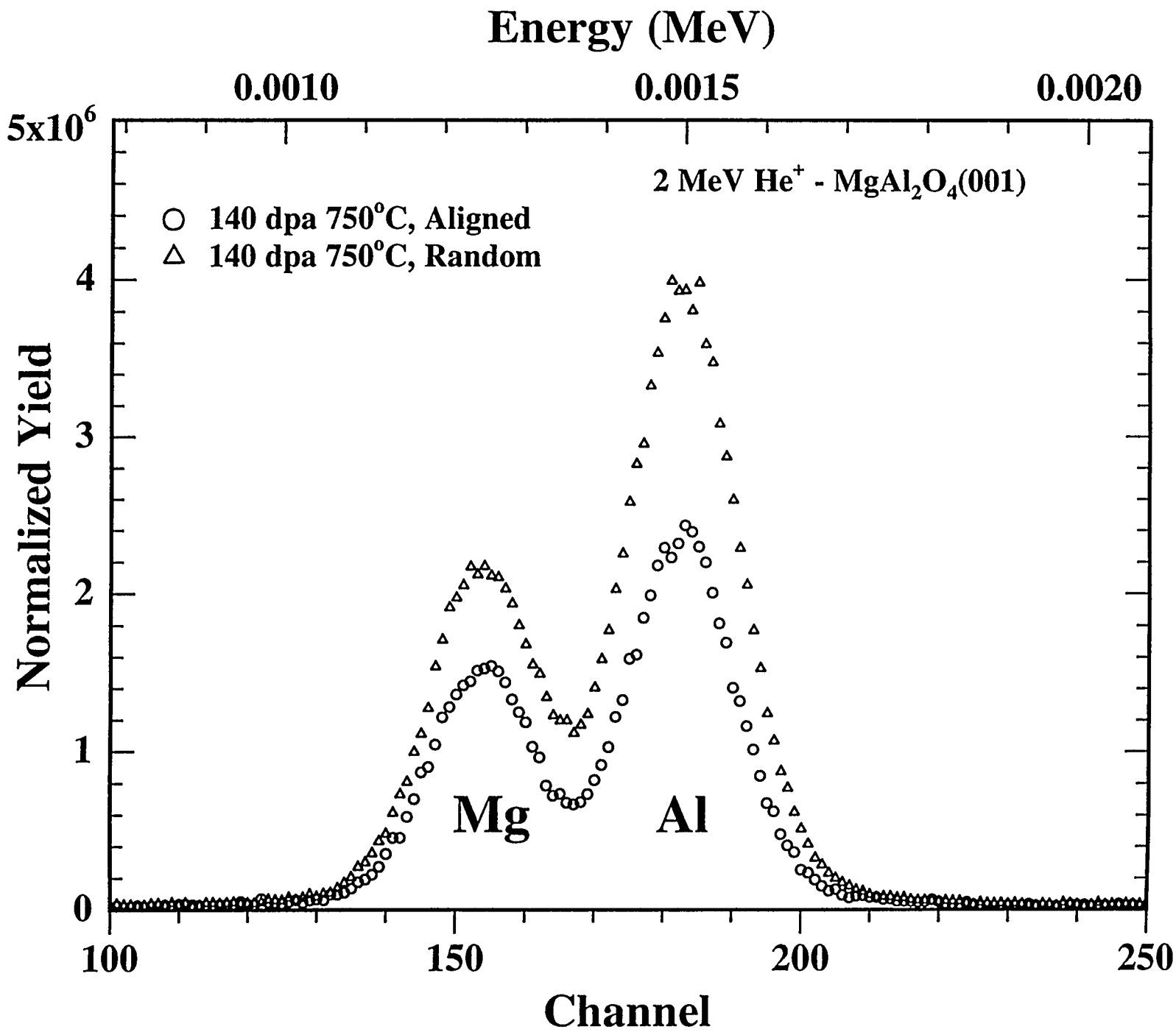
Energy (MeV)
0.0010
0.0015
0.0020
5x10^6
4
3
2
1
0
Normalized Yield
2 MeV He+ - MgAl2O4(001)
140 dpa 750°C, Aligned
140 dpa 750°C, Random
Mg
Al
100
150
200
250
Channel

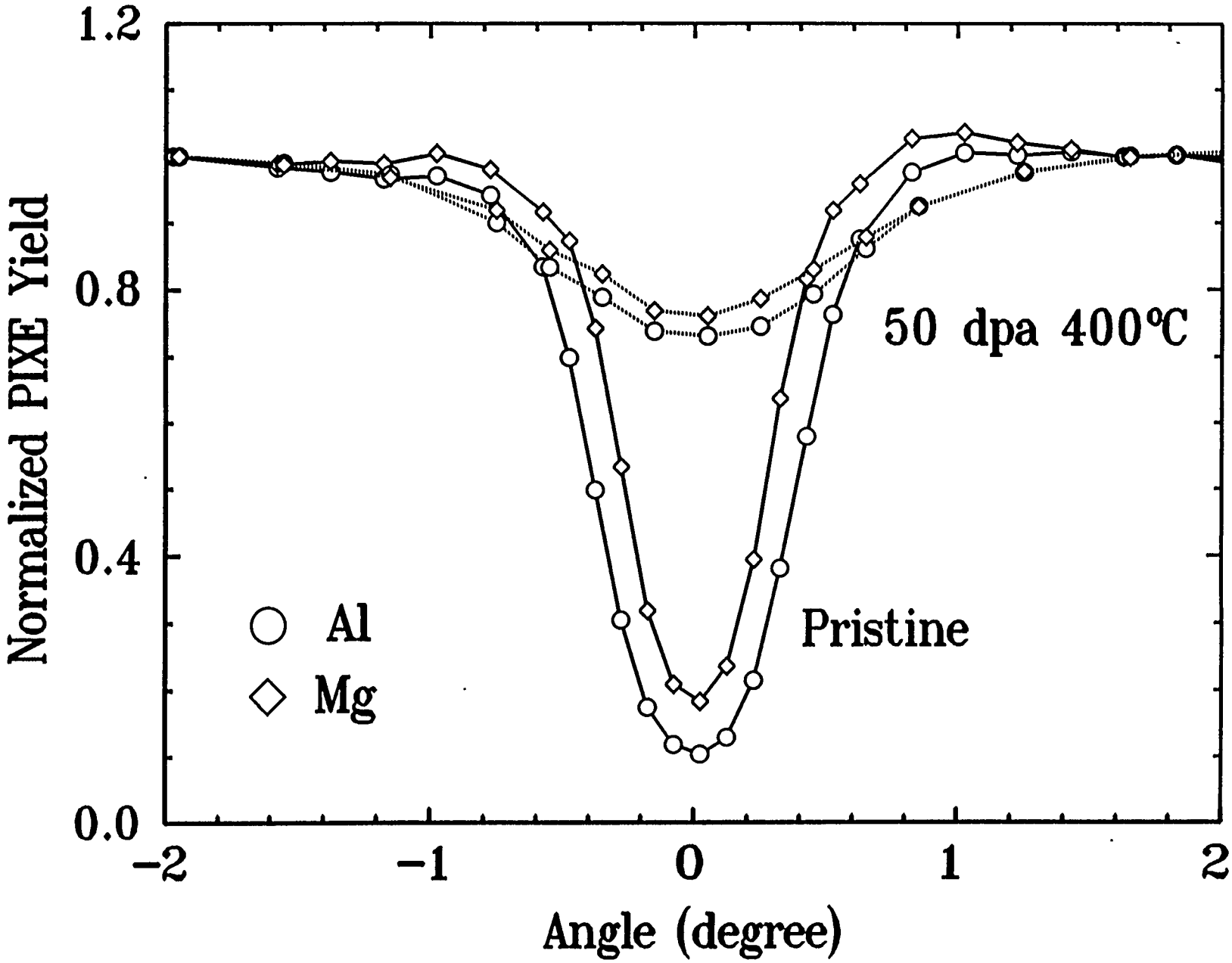
2 MeV He PIXE – $MgAl_2O_4$(100)
Normalized PIXE Yield
1.2
0.8
0.4
0.0
−2
−1
0
1
2
Angle (degree)
50 dpa 400°C
Al
Mg
Pristine

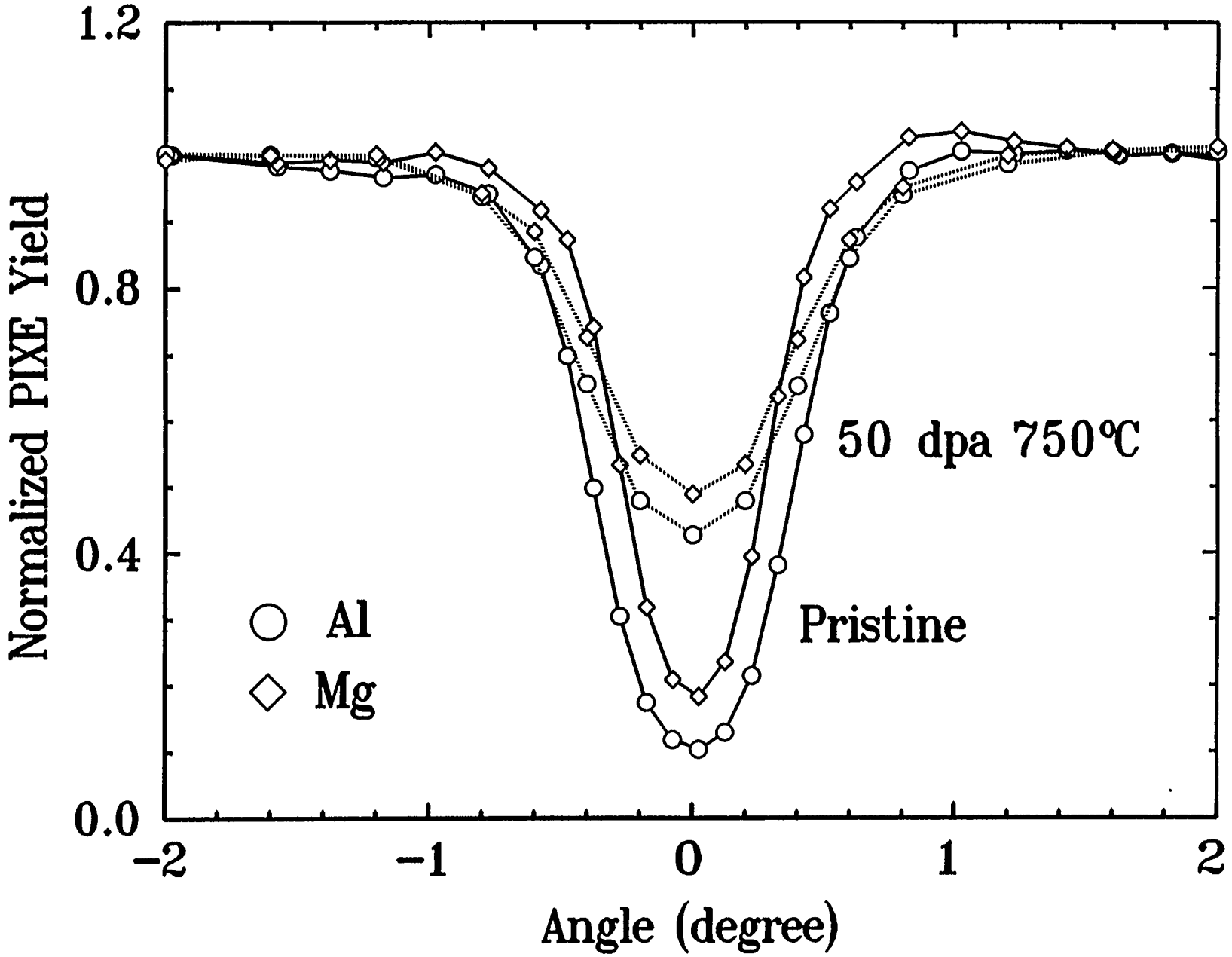
2 MeV He PIXE – $MgAl_2O_4$(100)
Normalized PIXE Yield
1.2
0.8
0.4
0.0
−2
−1
0
1
2
Angle (degree)
Al
Mg
50 dpa 750℃
Pristine